

# Engineering Notes

ENGINEERING NOTES are short manuscripts describing new developments or important results of a preliminary nature. These Notes cannot exceed 6 manuscript pages and 3 figures; a page of text may be substituted for a figure and vice versa. After informal review by the editors, they may be published within a few months of the date of receipt. Style requirements are the same as for regular contributions (see inside back cover).

AIAA 80-0736R

## Flutter Analysis of MBB A-3 Supercritical Airfoil in Small Disturbance Transonic Flow

T. Y. Yang,\* A. G. Striz,† and P. Guruswamy†  
Purdue University, West Lafayette, Ind.

### Introduction

IN recent years, there has been an increasing trend that aircraft be operated at speeds in the high subsonic or transonic regime. At these speeds, shocks form on the airfoil which result in an increase in the drag forces and a loss in lift force due to boundary layer separation. Consequently, to reduce such deficiencies, supercritical airfoils have been developed that can delay the drag rise Mach number and give higher lift coefficients.<sup>1-3</sup> In regard to steady aerodynamics, the supercritical airfoils have proven more efficient than conventional airfoils in the transonic regime. It is also of great practical interest to compare the unsteady aerodynamics. Farmer and Hanson<sup>4</sup> investigated two dynamically similar wings: one with a supercritical and the other with a conventional airfoil. The flutter boundaries were measured and compared with Kernel function calculations. The calculations agreed well with the wind tunnel tests up to  $M=0.85$  but did not indicate the large transonic dip. The flutter boundaries of the two wings were nearly identical up to  $M=0.9$ , after which the supercritical wing experienced a much more pronounced transonic dip. McGrew et al.<sup>5</sup> studied a TF-8A flutter model and the YC-15II prototype aircraft. These supercritical wings exhibited significantly lower flutter speeds than a conventional wing of equal size and rigidities. This agrees with the conclusions drawn in Ref. 4. Ashley<sup>6</sup> studied the flutter characteristics of a typical section of the TF-8A supercritical wing, 65.3% semispan station, using wind tunnel test results.<sup>7</sup> The influences of Mach number, section normal force coefficient, shock phase lag, and amplitude of shock displacement on flutter speeds for varying mass ratio were considered.

In these flutter analyses of supercritical airfoils, the aerodynamic data were obtained either from experiment, completely<sup>6</sup> or partially,<sup>5</sup> or from inviscid theory.<sup>4</sup> In the present flutter analysis of a MBB A-3 supercritical airfoil, designed by Messerschmitt-Bölkow-Blohm, theoretical aerodynamic data were used, obtained by two inviscid transonic computer codes: 1) LTRAN2 based on the time-integration method<sup>8</sup> with low-frequency approximation and 2) the steady and unsteady flow programs STRANS2 and UTRANS2, respectively, based on the harmonic method.<sup>9</sup> The unsteady aerodynamic data were obtained as the four aerodynamic coefficients  $C_{l_h}$ ,  $C_{l_{\alpha}}$ ,  $C_{m_h}$ , and  $C_{m_{\alpha}}$  by pitching

the airfoil about the  $1/4$ -chord axis for various values of low reduced frequencies ( $k_c < 0.2$ ).

The design conditions of the MBB A-3 supercritical airfoil are  $M=0.765$ , angle of attack  $\alpha=1.3$  deg, and steady lift coefficient  $C_l=0.58$ . From the steady pressure computations, it was found that at the design Mach number of 0.765 the angles of attack required to produce the design lift coefficient of 0.58 were 0.75 and 0.42 deg by STRANS2 and LTRAN2, respectively. Hence, the flutter analysis was performed at these equivalent conditions. The effects of various aeroelastic parameters, airfoil camber, and also of Mach number at zero angle of attack were investigated.

### Discussion

The parameters and sign conventions for the present two-degree-of-freedom airfoils are the same as those defined in Ref. 10. It is assumed that the airfoil is rigid, the amplitudes of oscillation are small, and that the principle of superposition for airloads is valid in the presence of shocks. The aeroelastic equations of motion and the equations for transformation of the aerodynamic coefficients can be found in Refs. 10 and 11. Three airfoil configurations are investigated: 1) a MBB A-3 supercritical airfoil; 2) a MBB A-3 airfoil with camber removed; and 3) a NACA 64A010 airfoil scaled down to 8.9% maximum thickness-to-chord ratio, the same as that of airfoil 1. The equations for these configurations were given by Olsen in private communication while the airfoil data are given in Ref. 12. Airfoils 2 and 3 are very similar. Flutter analyses were performed for design Mach number 0.765, design lift coefficient 0.58, and angles of attack 0.75 and 0.42 deg for STRANS2/UTRANS2 and LTRAN2, respectively.

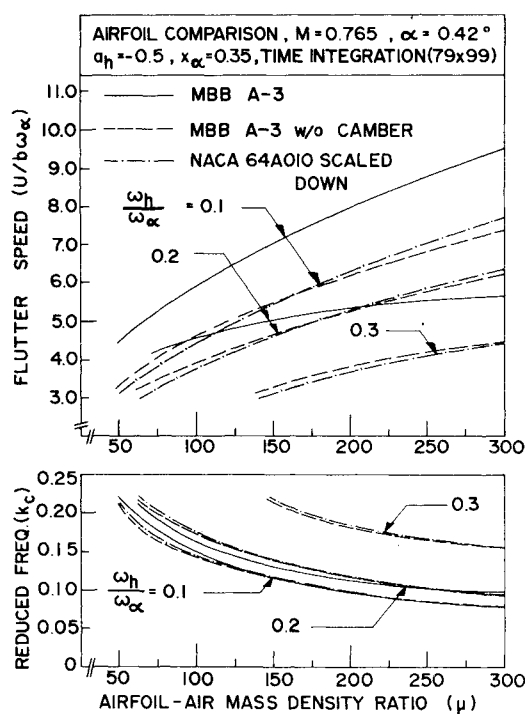


Fig. 1 Effect of airfoil-air mass density ratio on flutter speed by LTRAN2.

Presented as Paper 80-0736 at the AIAA/ASME/ASCE/AHS 21st Structures, Structural Dynamics and Materials Conference, Seattle, Wash., May 12-14, 1980; submitted June 9, 1980; revision received June 8, 1981. Copyright © American Institute of Aeronautics and Astronautics, Inc., 1980. All rights reserved.

\*Professor and Head, School of Aeronautics and Astronautics. Associate Fellow AIAA.

†Research Assistant, School of Aeronautics and Astronautics. Member AIAA.

For the steady computations, LTRAN2 was used in the SLOR-mode with Krupp scaling. STRANS2, which is based on a mixed-differencing relaxation procedure, was also used. The steady pressure distributions for all three airfoils, obtained by both codes, show that airfoil 1 experiences a shock, whereas airfoils 2 and 3 are subcritical.<sup>3,13</sup> The pressure curves for airfoils 2 and 3 are nearly the same, but the former have a little bump near the upper nose, possibly due to the blunter nose of airfoil 2 with supercritical thickness distribution. In general, the trends of the pressure curves obtained by LTRAN2 and STRANS2 agree well. The shock obtained by LTRAN2 is aft and stronger than that from

STRANS2, which can contribute to discrepancies in the unsteady coefficients.

The unsteady aerodynamic coefficients for the three airfoils obtained by both LTRAN2 and UTRANS2 are given in Refs. 3 and 13. The values for airfoil 1 are higher than those for airfoils 2 and 3, which are quite close. Both codes compare well in values and trends.

Based on the unsteady coefficients, flutter speeds were computed for the three airfoils by varying four parameters: airfoil-air mass density ratio  $\mu$ , location of mass center  $x_\alpha$ , plunge-pitch frequency ratio  $\omega_h/\omega_\alpha$ , and location of elastic axis  $a_h$ . The radius of gyration  $r_\alpha$  and reference frequency  $\omega_r$  were assumed as 0.5 and 1.0, respectively. Results are presented as six figures in Refs. 3 and 13. Two are presented here (Figs. 1 and 2). Both figures show that flutter speed increases steadily with the increase of the mass ratio. Removal of the camber shows an obvious destabilizing effect that reduces the flutter speed. On the other hand, the flutter characteristics of airfoils 2 and 3 are nearly identical.

Studies conducted earlier for several airfoils (see, for example, Refs. 4 and 10) have shown that the curve for flutter speed vs Mach number exhibits a dip in the transonic regime.

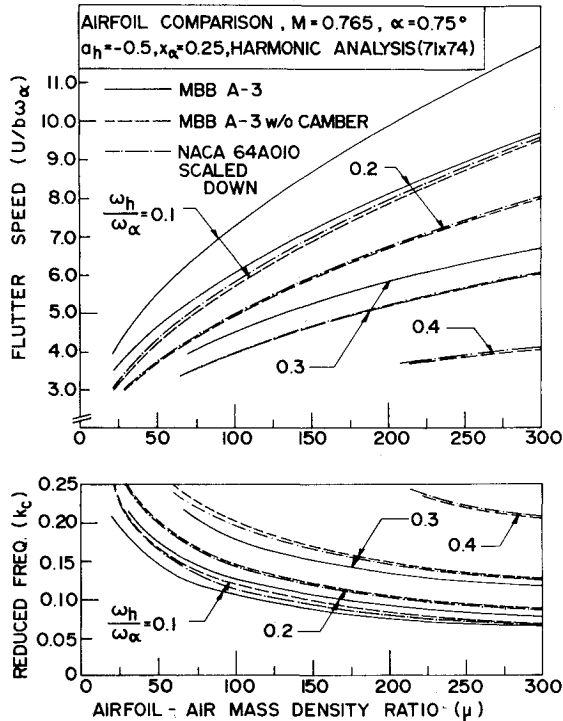


Fig. 2 Effect of airfoil-air mass density ratio on flutter speed by STRANS2/UTRANS2.

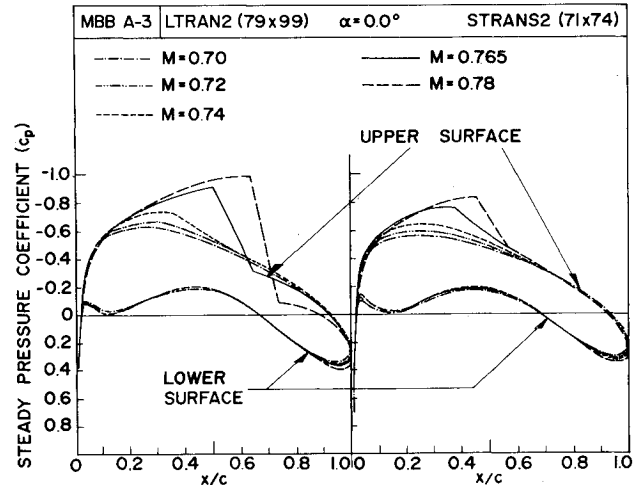


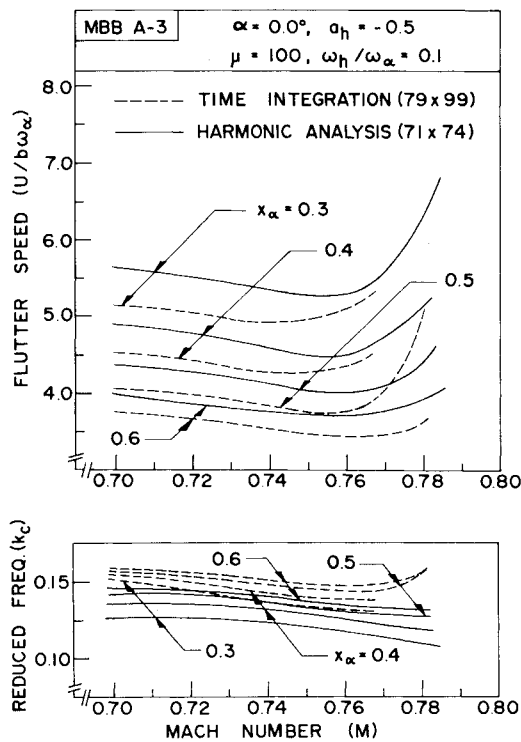
Fig. 3 Distribution of steady pressure coefficients.

Table 1 Aerodynamic coefficients for MBB A-3 airfoil for various Mach numbers at  $\alpha = 0.0$  deg by time integration (LTRAN2) with  $79 \times 99$  grid

Coefficient	Mach number	Reduced frequency, $k_c$							
		0.05		0.10		0.15		0.20	
		Real	Imag.	Real	Imag.	Real	Imag.	Real	Imag.
$C_{th}$	0.700	0.061	0.462	0.184	0.868	0.360	1.215	0.556	1.569
	0.720	0.077	0.483	0.215	0.897	0.404	1.244	0.592	1.543
	0.740	0.095	0.515	0.278	0.937	0.493	1.283	0.700	1.572
	0.765	0.171	0.636	0.422	1.100	0.724	1.420	0.881	1.728
	0.780	0.569	0.783	1.024	1.079	1.308	1.241	1.529	1.306
$C_{t\alpha}$	0.700	9.246	-1.217	8.677	-1.844	8.097	-2.398	7.845	-2.778
	0.720	9.652	-1.529	8.971	-2.154	8.296	-2.696	7.717	-2.962
	0.740	10.296	-1.908	9.374	-2.777	8.552	-3.283	7.862	-3.500
	0.765	12.724	-3.409	11.001	-4.223	9.469	-4.825	8.642	-4.403
	0.780	15.654	-11.373	10.794	-10.243	8.276	-8.721	6.531	-7.647
$C_{mh}$	0.700	0.002	-0.003	0.006	-0.007	0.011	-0.012	0.018	-0.020
	0.720	0.003	-0.003	0.007	-0.008	0.014	-0.015	0.020	-0.025
	0.740	0.003	-0.005	0.008	-0.012	0.016	-0.022	0.024	-0.036
	0.765	-0.008	-0.038	-0.015	-0.071	-0.022	-0.103	-0.029	-0.136
	0.780	-0.117	-0.144	-0.212	-0.172	-0.274	-0.178	-0.321	-0.164
$C_{m\alpha}$	0.700	-0.057	-0.037	-0.069	-0.056	-0.083	-0.075	-0.099	-0.089
	0.720	-0.062	-0.050	-0.077	-0.074	-0.101	-0.091	-0.126	-0.102
	0.740	-0.091	-0.059	-0.115	-0.083	-0.146	-0.106	-0.182	-0.118
	0.765	-0.763	0.162	-0.706	0.150	-0.686	0.146	-0.680	0.145
	0.780	-2.879	2.331	-1.719	2.122	-1.185	1.824	-0.818	1.606

**Table 2 Aerodynamic coefficients for MBB A-3 airfoil for various Mach numbers at  $\alpha = 0.0$  deg by harmonic analysis (UTRANS2) with  $71 \times 74$  grid**

Coefficient	Mach number	Reduced frequency, $k_c$									
		0.0		0.05		0.10		0.15		0.20	
		Real	Imag.	Real	Imag.	Real	Imag.	Real	Imag.	Real	Imag.
$C_{th}$	0.700	0.0	0.0	0.045	0.448	0.170	0.793	0.337	1.093	0.517	1.323
	0.720	0.0	0.0	0.060	0.456	0.195	0.818	0.379	1.116	0.579	1.328
	0.740	0.0	0.0	0.068	0.475	0.229	0.850	0.437	1.138	0.648	1.327
	0.765	0.0	0.0	0.089	0.521	0.260	0.900	0.523	1.185	0.772	1.288
	0.780	0.0	0.0	0.102	0.515	0.311	0.877	0.557	1.105	0.746	1.204
$C_{t\alpha}$	0.700	9.205	0.0	9.096	-0.560	7.971	-1.598	7.334	-1.869	6.749	-1.964
	0.720	9.598	0.0	8.961	-1.230	8.185	-1.803	7.469	-2.118	6.802	-2.202
	0.740	10.233	0.0	9.400	-1.450	8.487	-2.130	7.631	-2.441	6.864	-2.499
	0.765	11.221	0.0	10.141	-1.949	8.843	-2.801	7.667	-3.060	6.710	-2.970
	0.780	11.244	0.0	9.975	-2.047	8.664	-2.824	7.522	-3.068	6.514	-3.058
$C_{mh}$	0.700	0.0	0.0	0.002	-0.008	0.008	-0.017	0.016	-0.029	0.026	-0.042
	0.720	0.0	0.0	0.002	-0.009	0.009	-0.018	0.018	-0.030	0.028	-0.045
	0.740	0.0	0.0	0.003	-0.009	0.010	-0.019	0.020	-0.033	0.030	-0.050
	0.765	0.0	0.0	0.003	-0.015	0.010	-0.031	0.017	-0.053	0.020	-0.076
	0.780	0.0	0.0	-0.003	-0.034	-0.008	-0.063	-0.015	-0.090	-0.027	-0.112
$C_{m\alpha}$	0.700	-0.168	0.0	-0.171	-0.082	-0.175	-0.135	-0.188	-0.197	-0.202	-0.253
	0.720	-0.170	0.0	-0.172	-0.074	-0.182	-0.145	-0.199	-0.209	-0.216	-0.266
	0.740	-0.170	0.0	-0.173	-0.083	-0.189	-0.161	-0.211	-0.229	-0.235	-0.288
	0.765	-0.311	0.0	-0.307	-0.074	-0.319	-0.148	-0.340	-0.212	-0.365	-0.265
	0.780	-0.720	0.0	-0.663	0.025	-0.625	-0.002	-0.601	-0.037	-0.587	-0.054



**Fig. 4 Effect of Mach number on flutter speed for various mass center positions.**

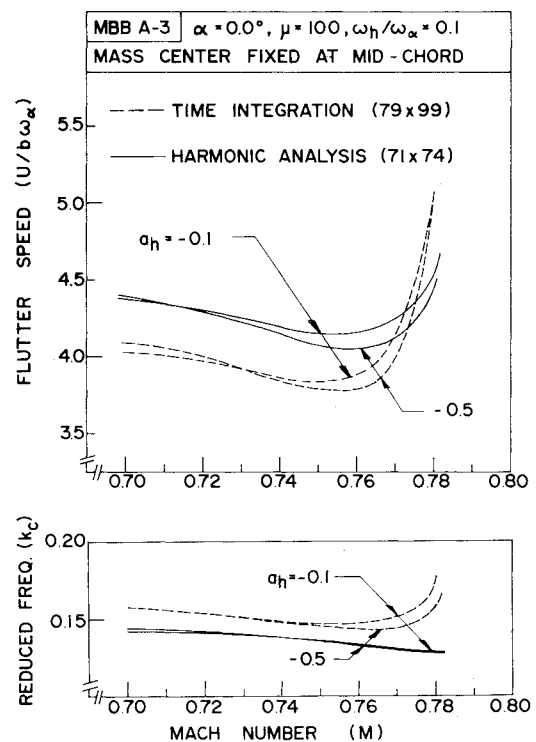


**Fig. 5 Effect of Mach number on flutter speed for two elastic axis positions.**

This transonic dip phenomenon was investigated for the MBB A-3 supercritical airfoil oscillating at zero mean angle of attack. Both programs LTRAN2 and STRANS2/UTRANS2 were used and the results are compared. The Mach numbers considered were 0.7, 0.72, 0.74, 0.765, and 0.78, respectively. The results for the steady pressure distributions are plotted in Fig. 3. The pressure curves on the upper surface grow rapidly with the increase in Mach number while those on the lower surface remain nearly unchanged. The shocks start to develop at Mach numbers between 0.74 and 0.765. The shocks ob-

tained by LTRAN2 are stronger and closer to the trailing edge than those by STRANS2.

Tables 1 and 2 show the unsteady aerodynamic coefficients obtained by LTRAN2 and UTRANS2, respectively. The agreement between the two tables is better at lower Mach numbers. Discrepancies may be attributed to 1) the basic difference in steady pressure curves, 2) different assumptions, and 3) different finite difference schemes.

Figures 4 and 5 show curves for flutter speed and the corresponding reduced frequency vs Mach number for dif-

ferent positions of the mass center and the elastic axis. Figure 4 shows that the flutter speed increases as the mass center moves forward, and Fig. 5 shows that the flutter speed does not change much as the position of the elastic axis changes from 45 to 25% chord measured from the leading edge.

In general, Figs. 4 and 5 demonstrate that the time-integration and harmonic analysis methods agree quite well. The agreement becomes less at higher Mach numbers. This difference stems from the lack of agreement in unsteady coefficients in Tables 1 and 2. All the curves show a dip in the neighborhood of the design Mach number.

### Acknowledgments

This research was sponsored under AFOSR Grant 78-3523A. The research was administered by L. J. Huttshell of AFWAL. Advice and help from J. J. Olsen and L. J. Huttshell of AFWAL, W. F. Ballhaus and P.M. Goorjian of NASA Ames, and S. R. Bland of NASA Langley are appreciated.

### References

- Whitcomb, R. T. and Clark, L. R., "An Airfoil Shape for Efficient Flight at Supercritical Mach Numbers," NASA TM X-1109 (confidential report), July 1965.
- Pearcey, H. H., "The Aerodynamic Design of Section Shapes for Swept Wings," *Advances in Aeronautical Sciences*, Vol. 3, 1962, pp. 277-322.
- Yang, T. Y., Guruswamy, P., and Striz, A. G., "Flutter Analysis of a Two-Dimensional and Two-Degree-of-Freedom Supercritical Airfoil in Small Disturbance Unsteady Transonic Flow," AFWAL-TR-80-3010, Air Force Wright Aeronautical Laboratories, March 1980.
- Farmer, M. G. and Hanson, P. W., "Comparison of Supercritical and Conventional Wing Flutter Characteristics," *Proceedings of the AIAA/ASME/SAE 17th Structures, Structural Dynamics, and Materials Conference*, King of Prussia, Pa., April 1976, pp. 608-611 (also NASA TM X-72837, May 1976).
- McGrew, J. A., Giesing, J. P., Pearson, R. M., Zuruddin, K., Schmidt, M. E., and Kalman, T. P., "Supercritical Wing Flutter," AFFDL-TR-78-37, Air Force Flight Dynamics Lab., March 1978.
- Ashley, H., "On the Role of Shocks in the 'Sub-Transonic' Flutter Phenomenon," *Journal of Aircraft*, Vol. 17, March 1980, pp. 187-197.
- Montoya, L. C. and Banner, R. D., "F-8 Supercritical Wing Flight Pressure, Boundary Layer, and Wake Measurements and Comparisons with Wind Tunnel Data," NASA TM X-3544, June 1977.
- Ballhaus, W. F. and Goorjian, P. M., "Implicit Finite Difference Computations of Unsteady Transonic Flows about Airfoils Including the Treatment of Irregular Shock-Wave Motions," AIAA Paper 77-205 (also *AIAA Journal*, Vol. 15, Dec. 1977, pp. 1728-1735).
- Traci, R. M., Albano, E. D., and Farr, J. L. Jr., "Perturbation Method for Transonic Flows about Oscillating Airfoils," *AIAA Journal*, Vol. 14, Sept. 1976, pp. 1258-1265.
- Yang, T. Y., Guruswamy, P., Striz, A. G., and Olsen, J. J., "Flutter Analysis of a NACA 64A006 Airfoil in Small Disturbance Transonic Flow," *Journal of Aircraft*, Vol. 17, April 1980, pp. 225-232.
- Traci, R. M., Albano, E. D., and Farr, J. L. Jr., "Small Disturbance Transonic Flows About Oscillating Airfoils and Planar Wings," AFFDL-TR-75-100, Air Force Flight Dynamics Lab., June 1975.
- Olsen, J. J., "AGARD Standard Configurations for Aeroelastic Applications of Transonic Unsteady Aerodynamics, Part III, Candidate Airfoil Data," AFFDL-TM-78-6-FBR, Air Force Flight Dynamics Lab., Jan. 1978.
- Yang, T. Y., Striz, A. G., and Guruswamy, P., "Flutter Analysis of a Two-Degree-of-Freedom MBB A-3 Supercritical Airfoil in Two-Dimensional Transonic Flow," *Proceedings of the AIAA/ASME/ASCE/AHS 21st Structures, Structural Dynamics, and Materials Conference*, Seattle, Wash., May 1980, pp. 434-443.

AIAA 81-4268

## Prediction of Range and Endurance of Jet Aircraft at Constant Altitude

Charles W. Bert\*

University of Oklahoma, Norman, Okla.

### Nomenclature

$a_i$	= coefficients defined in Eqs. (13); $i = -3, -1, 1$
$a, b$	= constants defined in Eqs. (9)
$C$	= thrust specific fuel consumption
$C_0, C_1$	= zeroth- and first-order thrust coefficients of fuel consumption
$C_D, C_L$	= total drag and lift coefficients
$C_{D_0}$	= parasite-drag coefficient
$D$	= total aerodynamic drag force
$E$	= endurance
$K$	= induced-drag factor
$L$	= aerodynamic lift force
$q$	= dynamic pressure
$R, R_s$	= cruising range, specific range
$(R_s)_{\max}$	= maximum value of specific range
$S$	= wing area
$T, t$	= thrust force and time
$V, V_{md}$	= true airspeed at cruise and for minimum drag
$V_{\text{opt}}$	= true airspeed for maximum range
$W, \dot{W}$	= aircraft gross weight and its time derivative
$W_f, W_i$	= final and initial values of $W$
$\rho$	= atmospheric density at cruising altitude

### Introduction

WITH the cost of petroleum-based fuels continuing to spiral upward, the subject of range and endurance vs fuel economy has taken on renewed importance. Thus, the precise manner in which range and endurance are predicted is becoming more crucial. Perhaps the first published analyses of range for turbojet-powered aircraft (there were undoubtedly numerous early analyses of an unpublished nature, such as company reports, etc.) were those of Page<sup>1</sup> and Jonas,<sup>2</sup> both in 1947. However, Page was concerned with only specific range rather than total. Jonas derived the square-root range expression (see Appendix A). In deriving this equation, he assumed that angle of attack is maintained at that required for maximum range and that engine speed and airspeed are decreased as fuel is consumed in the course of the flight. The same form of equation was derived in the well-known textbooks of Perkins and Hage<sup>3</sup> and Dommasch et al.<sup>4</sup>

Reference 2 was followed by the work of Ashkenas,<sup>5</sup> who obtained a similar expression for jet-aircraft range at altitudes below 35,000 ft and a logarithmic form (see Appendix B)<sup>6-12</sup> for the constant-temperature stratosphere.

It is shown here that neither the square-root (Appendix A) nor the logarithmic (Appendix B) form are appropriate for constant-altitude cruise because of the following.

1) The assumption that the thrust specific fuel consumption ( $C$ ) is constant, regardless of thrust level, is a poor representation of actual turbojet or turbofan characteristics.

2) At constant altitude, the sets of variables ( $\rho, C, C_L^{1/2}/C_D$ ) or ( $C, L/D, V$ ) cannot be held constant when  $W$  is changing. However, both Ashkenas<sup>5</sup> and Nicolai<sup>10</sup> noted that the latter set can be held constant in a cruise climb by holding

Received Aug. 16, 1980; revision received March 30, 1981. Copyright © American Institute of Aeronautics and Astronautics, Inc., 1980. All rights reserved.

\*Benjamin H. Perkinson Professor of Engineering, School of Aerospace, Mechanical and Nuclear Engineering. Associate Fellow AIAA.